ACS OMEGA

http://pubs.acs.org/journal/acsodf

Article

Three-Dimensional Supramolecular Architectures with Mn^{II} Ions Assembled from Hydrogen Bonding Interactions: Crystal Structures and Antiferromagnetic Properties

Yan-Li Gao,* Yufei Wang, Liguo Gao, Jian Li, Yali Wang, and Katsuya Inoue*

Cite This: *ACS Omega* 2022, 7, 10022−10028

Read Online

ACCESS | Metrics & More | Article Recommendations | Supporting Information

ABSTRACT: Two novel cocrystal Mn^{II} compounds were successfully synthesized. The composition of two kinds crystals correspond to $[Mn(hfac)_2L^a_2{\cdot}Mn(hfac)_2L^a(H_2O){\cdot}Mn(hfac)_2(H_2O)_2]$ (**1**) and $[Mn(hfac)_2L^b_2{\cdot}Mn(hfac)_2(H_2O)_2{\cdot}0.5(C_6H_{14})]$ (**2**) [L^a = 1,3-bis(1′-oxyl-3′-oxido-4′,4′,5′,5′-tetramethyl-4,5-dihydro-1*H*-imidazol-2-y1)benzene; L^b = 1-(1′-oxyl-4′,4′,5′,5′-tetramethylimidazolin-2-yl)-3-(1′-oxyl-3′-oxo-4′,4′,5′,5′-tetramethylimidazolin-2-yl)benzene; hfac = hexafluoroacetylacetonato). Surprisingly, the compounds were not polymeric or clusters but, more interestingly, different ratio biradical−metal coordination compound cocrystals. The extensive intramolecular H-bonds are the cause of formation of the cocrystal structures by assembly in the two manganese(II) derivatives; and another factor is the halogen bonds between CF_3 of hfac groups. Furthermore, three-dimensional supramolecular architectures were formed. The magnetic susceptibility of both compounds showed strong antiferromagnetic interactions involving the coordinated radical unit and the metal and lesser contribution from ferromagnetic interactions between the radical units. For compound **1**, a good fit was obtained for g_{Mn} = 2.08, g_{rad} = 2.00 (fixed), J_1 = −294.3 cm^{-1}, J_2 = 6.2 cm^{-1} and J_3 = 10.8 cm^{-1}. A reasonable fit for compound **2** was obtained for g_{Mn} = 2.04, g_{rad} = 2.00 (fixed), J_1' = −273.4 cm^{-1} and J_2' = 8.6 cm^{-1}.

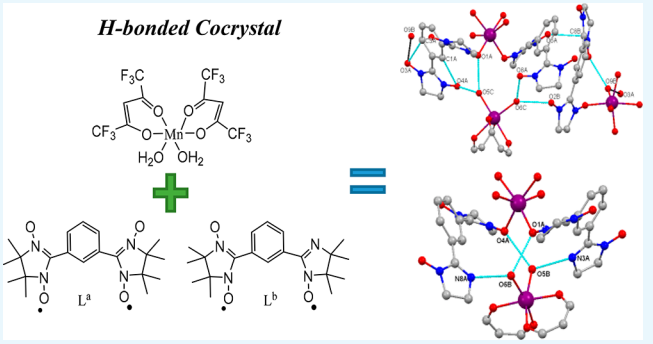

INTRODUCTION

In past years, the syntheses and study of molecular-based magnetic materials have always been an object of interest to scholars, in part because they may eventually be used in molecular electronics devices.[1] Combining paramagnetic organic compounds and transition metals produces multifarious complexes through the so-called metal−radical strategy that have different crystalline structures and magnetic properties.[2−5] In particular, the most widely studied radicals in this strategy are nitronyl nitroxides[6] because of their excellent stability, easy synthesis and chemical modification, and ability to bridge the ligands and metal centers.[7,8] The strategy has been incredibly successful, and a variety of species combining nitronyl nitroxides with transition metal ions have been described.[9,10]

Organic biradicals as building blocks for molecular-based magnetic materials have attracted great interest,[11] in part because there is the possibility to change the ground spin state by selecting a suitable conjugated spacer between the groups with unpaired spin. One of the most used spacers is the *m*-phenylene ring due to its non-disjointed connectivity, which induces an S = 1 spin ground state for many biradicals.[12,13] Iminoylnitroxide (INR) is a much-less-utilized analog as a bridge to form coordination complexes in the metal−radical approach. Many possibilities remain unexplored using these spin carriers to alter the coordination structural and magnetic behavior because few coordination compounds containing INR type biradicals have been reported.[14,15]

Co-crystallization is a major aspect of crystal engineering. It has important applications in the development and manufacture of pharmaceutical products,[16−18] but is rarely invoked in the research of magnetic materials.[19,20] We produced two biradicals,[21−23] NIT-Ph-(3-NIT), (L^a) and NIT-Ph-(3-NI), (L^b) (Scheme 1), and studied their reaction with manganese compounds (Figure 1). Two cocrystal metal−radical compounds, $[Mn(hfac)_2L^a_2{\cdot}Mn(hfac)_2L^a(H_2O){\cdot}Mn(hfac)_2(H_2O)_2]$ (**1**) and $[Mn(hfac)_2L^b_2{\cdot}Mn(hfac)_2(H_2O)_2{\cdot}0.5(C_6H_{14})]$ (**2**), were attained and their single crystals were studied (Figure 1). Surprisingly, these compounds were not polymeric or clusters but, more interestingly, different ratio biradical−metal coordination compound cocrystals,[24−27]

Received: September 24, 2021
Accepted: March 4, 2022
Published: March 15, 2022

https://doi.org/10.1021/acsomega.1c05285
ACS Omega 2022, 7, 10022−10028

Scheme 1. Structures of Nitronyl Nitroxide Radicals NIT-Ph-(3-NIT) (L^a) and NIT-Ph-(3-NI) (L^b)

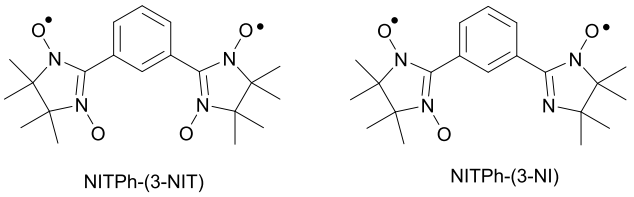

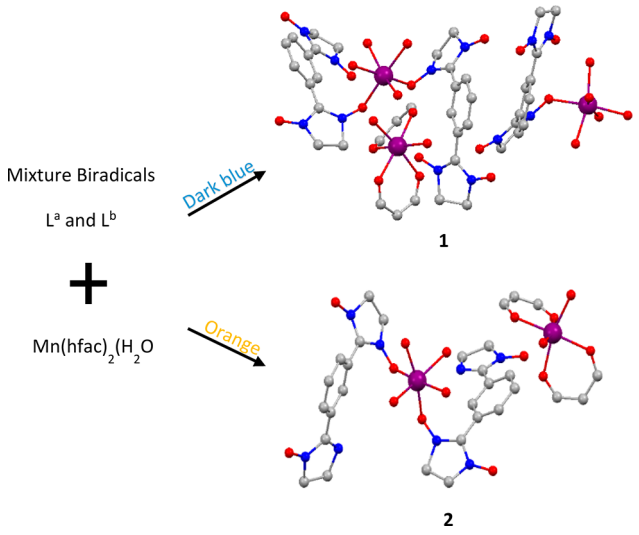

Figure 1. Synthesis and structures of the Mn(II) compounds **1** and **2**. All hydrogen and fluorine atoms, part of the carbon atoms of hfac ligands, and the methyl of the biradical were omitted for the sake of clarity.

which have been rarely reported as magnetic materials.[28−30] The magnetism of the two compounds was evaluated finally.

RESULTS AND DISCUSSION

Crystal Structure of Complexes 1 and 2. The air-stable biradical and the tri- and binuclear Mn cocrystals **1** and **2** can be synthesized conveniently. Compounds **1** and **2** were characterized by single crystal X-ray diffraction analyses (Table 1). In both compounds the metal centers are in a weakly distorted pseudo-octahedral coordination environment. Selected bond lengths, angles and torsion angles are listed in Table 2 and Tables S1 and S2 (ESI), and they are typical for Mn^{II} ions coordinated to $hfac^-$ and N−O groups.[19−21] It is worth noting that, although the radicals L^a and L^b both have two N−O groups available for coordination, they act only as a monodentate ligands in **1** and **2**, leaving one spin site uncoordinated.

Compound **1** crystallized in monoclinic space group *C*2/*c* with three unique Mn^{II} centers in the asymmetric unit (Figure 2). In the cocrystallized structure, there are three distinct complexes, namely, $[Mn(hfac)_2L^a_2]$ (A), $[Mn(hfac)_2L^a(H_2O)]$ (B), and $[Mn(hfac)_2(H_2O)_2]$ (C). In fragment A, the composition corresponds to one $Mn(hfac)_2$ and two *cis*-coordinated biradical L^a. The Mn1A ion is coordinated to four oxygen atoms (O9A, O10A, O11A, and O12A) of two hfac groups and two oxygen atoms (O1A and O5A) from two bis(nitronyl nitroxide) L^a. In fragment B, the composition corresponds to one $Mn(hfac)_2$, one *cis*-coordinated biradical L^a, and one water molecule. The Mn1B ion is coordinated to four oxygen atoms (O5B, O6B, O7B, and O8B) from two $hfac^-$ groups plus two oxygen atoms from one bis(nitronyl nitroxide) radical (O1A) and one water molecule (O9B). In comparison, in fragment C, the Mn1C ion is coordinated to six oxygen atoms which are from two hfac groups (O1C, O2C, O3C, and O4C) plus two *cis*-coordinated water molecules (O5C and O6C). The nitroxide−metal bond angles N1A−

Table 1. Crystallographic Data of Compounds 1 and 2 at 123 K

	1	2
formula	$C_{90}H_{96}F_{36}Mn_3N_{12}O_{27}$	$C_{63}H_{71}F_{24}Mn_2N_8O_{15}$
fw	2626.60	1746.15
cryst syst	monoclinic	triclinic
space group	*C*2/*c*	$P\bar{1}$
a (Å)	34.766(3)	12.8709(6)
b (Å)	15.7586(11)	14.7145(7)
c (Å)	40.899(3)	23.2599(11)
α (deg)	90.00	75.319(2)
β (deg)	97.383(2)	74.2760(10)
γ (deg)	90.00	77.750(2)
V (Å^3)	22221(3)	4052.9(3)
Z	8	2
ρ_{calcd} (g cm^{-3})	1.570	1.431
F(000)	10680	1782
θ range (deg)	2.787−28.357	2.766−28.37
reflns total	278214	150472
unique/params	14207/1594	10875/1089
R_{int}	0.1617	0.0451
R_1/wR_2 [$I > 2\sigma(I)$]	0.081/0.1837	0.0916/0.2602
R_1/wR_2 (all data)	0.1726/0.2124	0.1647/0.3130
completeness	0.996	0.995
GoF	1.023	1.021

Table 2. Selected Bond Lengths (Å) for Compounds 1 and 2

bond	length	bond	length
	1		
N1A−O1A	1.323(4)	N7A−O7A	1.277(5)
N2A−O2A	1.263(5)	N8A−O8A	1.289(5)
N3A−O3A	1.298(5)	N1B−O1B	1.291(4)
N4A−O4A	1.260(5)	N2B−O2B	1.289(4)
N5A−O5A	1.307(4)	N3B−O3B	1.279(5)
N6A−O6A	1.250(4)	N4B−O4B	1.285(5)
Mn1A−O1A	2.125(3)	Mn1B−O7B	2.182(3)
Mn1A−O5A	2.132(3)	Mn1B−O8B	2.158(3)
Mn1A−O9A	2.184(3)	Mn1B−O9B	2.163(3)
Mn1A−O10A	2.161(3)	Mn1C−O1C	2.163(3)
Mn1A−O11A	2.184(3)	Mn1C−O2C	2.177(3)
Mn1A−O12A	2.152(3)	Mn1C−O3C	2.175(3)
Mn1B−O1B	2.148(3)	Mn1C−O4C	2.176(3)
Mn1B−O5B	2.158(3)	Mn1C−O5C	2.146(3)
Mn1B−O6B	2.169(3)	Mn1C−O6C	2.144(4)
	2		
N1−O1	1.330(4)	N5−O4	1.328(4)
N2−O2	1.296(8)	N6−O5	1.259(9)
N4−O3	1.268(6)	N7−O6	1.261(8)
Mn1−O1	2.145(3)	Mn2−O11	2.172(3)
Mn1−O4	2.163(3)	Mn2−O12	2.152(4)
Mn1−O7	2.170(3)	Mn2−O13	2.143(4)
Mn1−O8	2.159(3)	Mn2−O14	2.156(4)
Mn1−O9	2.180(3)	Mn2−O15	2.163(3)
Mn1−O10	2.178(3)	Mn2−O16	2.157(3)

https://doi.org/10.1021/acsomega.1c05285
ACS Omega 2022, 7, 10022−10028

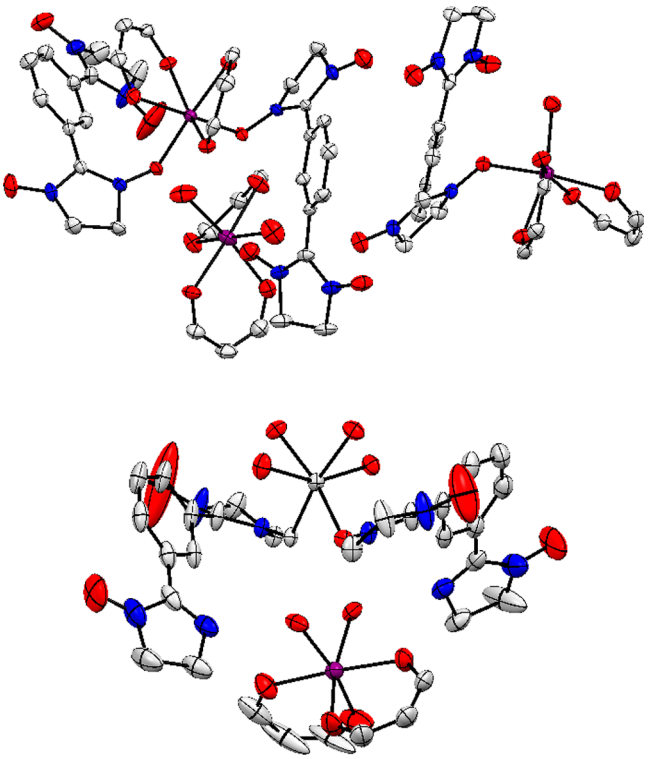

Figure 2. Coordination environment of compounds **1** (top) and **2** (bottom) with 50% ellipsoid probability. All fluorine and hydrogen atoms, part of the carbon atoms of hfac ligands, and the methyl of the biradicals were omitted for the sake of clarity.

O1A−Mn1A, N5A−O5A−Mn1A, and N1B−O1B−Mn1B in compound **1** are 123.51°, 118.23°, and 128.60°, respectively. These are typical angles of compounds of coordinated nitronyl nitroxide groups and manganese ions.[31,32] The torsion angles between the imidazolyl and phenyl rings are smaller than 50° (Table S1, ESI).

In stabilizing the crystal packing, the water molecule of crystallization plays a crucial role by participating in a H-bond network, which is shown in Figure 3a and Figure S2 (ESI). In addition, forked H-bonds of fragments A, B, and C are probably a driving force to cocrystallize these three different fragments. The distances between the acceptor and donor atoms in these H-bonds of compound **1** are 2.649 Å (O6C−O8A), 2.698 Å (O4A−O5C), 2.783 Å (O6C−O2B), 2.801 Å (O4B−O9B), 2.846 Å (O1A−O5C), and 2.874 Å (O3A−O9B). Intermolecular halogen contacts F3A−F2C (2.811 Å), F11C−F11C (2.905 Å), and F11A−F2B (2.990 Å) and oxygen contacts O2A−O3A (3.073 Å) are observed between the molecular units, as depicted in Figure 3b, which links the neighboring molecules to form layers. Furthermore, those bonds lead to alternating supramolecular pseudohelices, which drive the formation of such 3D structures (Figure 3c). A few short intra- and intermolecular contacts are also observed at distances of 2.882 Å (O3A−C3A), 2.883 Å (O4A−C1A), 2.883 Å (O6A−C8B), and so on.

Compound **2** crystallized in triclinic space group $P\bar{1}$ including two unique Mn^{II} centers in an asymmetric unit. The asymmetric units of **2** are shown in Figure 2 (bottom) and Figure S3 (ESI). There are two distinct complexes cocrystallized in each crystal structure, namely $[Mn(hfac)_2L^b{}_2]$ (A) and $[Mn(hfac)_2(H_2O)_2]$ (B). Bond lengths listed in Table 2 are typical for Mn(II) ions coordinated to hfac and N−O groups.[33] The nitroxide−metal bond angles, N1A−O1A−Mn1A and N5A−O4A−Mn1A. are slightly smaller in compound **2** (123.47° and 120.80°) than in cocrystal **1**. The torsion angles between the imidazolyl and phenyl rings are smaller than 50° (Table S2, ESI).

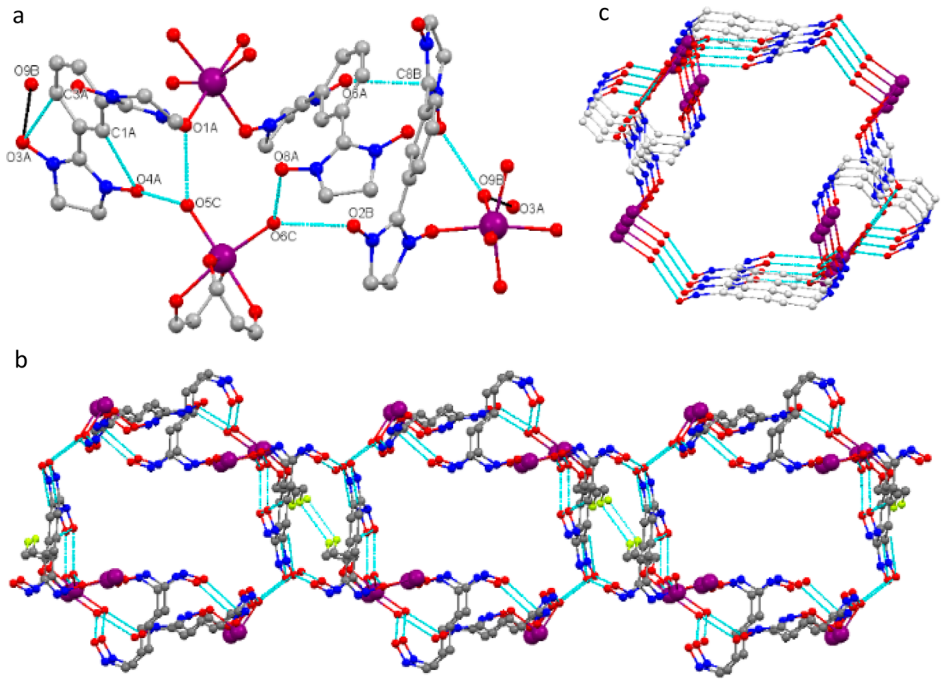

Figure 3. Crystal packing of compound **1**. (a) Intra- and intermolecular H-bonds. (b) H-bonds among cocrystal oxygen atoms and short contacts F···F. (c) Displayed helical sublattices through H-bonds. All fluorine and hydrogen atoms, part of the carbon atoms of the hfac ligands, and the methyl of the biradical were omitted for the sake of clarity.

https://doi.org/10.1021/acsomega.1c05285
ACS Omega 2022, 7, 10022−10028

The crystallization water molecule plays a similar role to that in cocrystal **1**. The distances between oxygen atoms in these H-bonds for compound **2** and intermolecular halogen contacts were also obtained, as depicted in Figure S4 (ESI), leading to an alternating supramolecular pseudolayer, which is like a butterfly.

The UV/vis absorption spectra of the two metal complexes are shown in Figure 4. The cocrystal **1** shows three typical

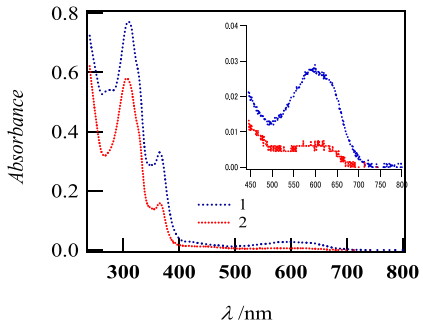

Figure 4. UV/vis spectrum of 0.1 mmol L^{-1} **1** and **2** in CH_2Cl_2. The inset shows a magnification of the 450 to 800 nm region.

transitions approximately at wavelengths 310, 365, and 580 nm, which correspond to an α-nitronyl nitroxide radical (blue trace). These originated from the $\pi\pi^*$-transitions of the phenyl ring with high intensity, $\pi\pi^*$-transition of the NO group with middle intensity, and broad $n\pi^*$-transition of the NO group with low intensity, respectively.[34] No absorption peak was observed at wavelengths longer than 700 nm, suggesting no intervalence absorption. These results suggest that an unpaired electron is localized on the NIT ring. Cocrystal **2** had similar absorptions around 306 and 365 nm but weak absorption observed around 580 nm. These results indicate that the uncoordinated spin site is the NI ring.

Magnetic Properties. The magnetic susceptibilities of compounds **1** and **2** were measured on polycrystalline samples in an applied field of 5 kOe, and the data were corrected for the diamagnetism of the contents (Figure 5 and 6).

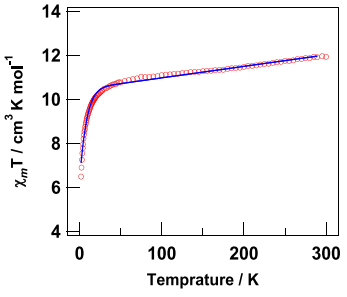

Figure 5. Temperature dependence of the product of magnetic susceptibility ($\chi_m T$) for **1** (red). The solid blue line corresponds to the best fit.

For compound **1** (Figure 5), the $\chi_m T$ experimental value at 300 K is only 11.95 cm^3 K mol^{-1}, which is lower than the calculated value (15.6 cm^3 K mol^{-1}) for three noninteracting Mn(II) ions ($S = 5/2$) plus six nitronyl nitroxide radicals (each $S = 1/2$) with $g = 2$. This value suggests that strong antiferromagnetic exchange interactions exist at room temperature. Following cooling, the $\chi_m T$ value decreases gradually before around 30 K. The $\chi_m T$ value is ca. 10.4 cm^3 K mol^{-1} at

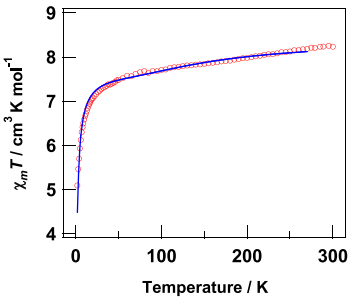

Figure 6. Temperature dependence of the product of magnetic susceptibility ($\chi_m T$) for **2** (red). The blue solid line corresponds to the best fit.

this temperature and corresponds to three $S = 1/2$ spins, one $S = 3/2$, one $S = 2$, and one $S = 5/2$ assuming $g = 2.00$. Then upon cooling, a strong drop was observed, and $\chi_m T$ is 6.46 cm^3 K mol^{-1} at 2 K. Below 30 K, the decrease of $\chi_m T$ can be attributed to intermolecular antiferromagnetic interactions. Parameters C and θ were estimated to be 11.81 cm^3 K mol^{-1} and −3.9 K by the Curie−Weiss fit of the $\chi^{-1}(T)$ curve (solid red line in Figure S5, ESI).

In order to account for the magnetic behavior of compound **1**, it is possible to use a simplified model with two coupling constants to describe the magnetic behavior since the proposed path was the same in both units of fragment A. When four magnetic coupling constants were used, the experimental uncertainty of J increased strongly, leading to a meaningless result (Scheme 2), where J_1 and J_2 represent the magnetic

Scheme 2. Two Exchange Coupling Constants Model Used to Fit the Magnetic Data of Compounds 1

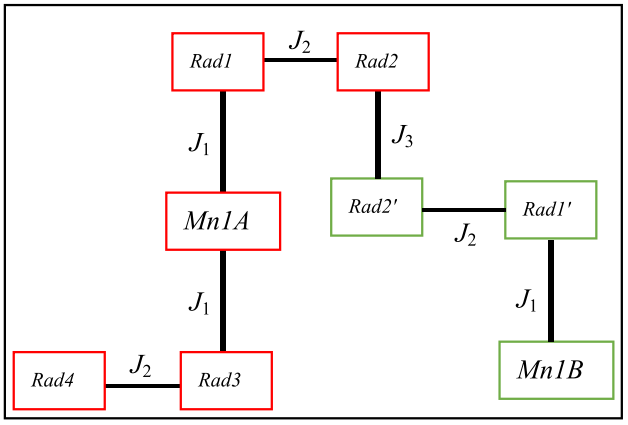

interactions of coordinated metal−radical and that within the biradical (radical−radical), respectively. Despite a wealth of short intermolecular contacts of O6A to O3B (3.398 Å) in complexes **1**, the magnetic exchange coupling between fragment A and B should be weak when compared to the interactions within the Mn-radical. In addition, the closest intermolecular contact involving significant spin density sites does not give substantial radical−radical singly occupied molecular orbital SOMO−SOMO overlap, so it will result in a small exchange contribution.[22−24]

Through the crystal structure, the magnetic interaction mainly arises from three pathways: magnetic exchange interaction between the Mn^{II} ion and the directly coordinated NO group (J_1) (containing part A and part B); magnetic

https://doi.org/10.1021/acsomega.1c05285
ACS Omega 2022, 7, 10022−10028

exchange interaction between two NO groups through the *m*-phenylene ring (J_2) that also includes components A and B; magnetic coupling between part A and B through the intermolecular noncovalent NO···ON contacts (J_3). Hence, the magnetic data were considered a sum of the magnetic susceptibility corresponding to the spin Hamiltonian:[35]

$$[H = -J_1(S_{Rad1}\cdot S_{Mn1A} + S_{Rad3}\cdot S_{Mn1A} + S_{Rad1'}\cdot S_{Mn1B}) - J_2(S_{Rad1}\cdot S_{Rad2} + S_{Rad3}\cdot S_{Rad4} + S_{Rad1'}\cdot S_{Rad2'}) - J_3(S_{Rad2}\cdot S_{Rad2'}) + Dz]$$

The magnetically isolated Mn^{II} ion (Mn1C) was included in the Hamiltonian only as the Zeeman component (Dz). The best fit was achieved with $g_{Mn} = 2.08$, $g_{rad} = 2.00$ (fixed), $J_1 = -294.3$ cm^{-1}, $J_2 = 6.2$ cm^{-1}, and $J_3 = 10.8$ cm^{-1} (solid blue line in Figure 5).[36,37] The torsion angle between the *m*-phenylene spacer and imidazolyl rings plays a major role in the intramolecular exchange interactions between the nitroxide spins.

Furthermore, the magnetization reaches only 10 Nμ_B at 50 kOe, far from saturated value (Figure S6, ESI). These results, including the room temperature $\chi_m T$ value, low temperature $\chi_m T$ value, low M value at 50 kOe, negative Weiss constant, and negative J_1 value suggest the existence of significant antiferromagnetic interactions between the spins, which is consistent with the literature results for the Mn−Rad systems.[38−41]

Compound **2** presents qualitatively similar magnetic behavior to **1**, with the thermal dependence of $\chi_m T$ product shown in Figure 6 (red). At 300 K, the experimental value of $\chi_m T$ is 8.23 cm^3 K mol^{-1}, significantly lower than the expected value for uncorrelated spins (10.2 cm^3 K mol^{-1} if all $g = 2.0$), which indicates strong antiferromagnetic exchange interactions. Upon cooling, the $\chi_m T$ value decreases gradually until around 20 K; the $\chi_m T$ value of 7.07 cm^3 K mol^{-1} corresponds to two $S = 1/2$ spins, one $S = 3/2$, and one $S = 5/2$ assuming $g = 2.00$. Then a strong drop was observed to 5.09 cm^3 K mol^{-1} at 2 K after the temperature decreased. The Curie and Weiss constants were estimated to be 8.21 cm^3 K mol^{-1} and −4.2 K by the Curie−Weiss fit of the $\chi_m^{-1}(T)$ curve (Figure S5, ESI). The solid blue line in Figure 6 shows the best fit using the spin Hamiltonian of $H = -J_1'(S_{Rad1}\cdot S_{Mn1A} + S_{Rad3}\cdot S_{Mn1A}) - J_2'(S_{Rad1}\cdot S_{Rad2} + S_{Rad3}\cdot S_{Rad4}) + Dz']$ achieved with $g_{Mn} = 2.04$, $g_{rad} = 2.00$ (fixed), $J_1' = -273.4$ cm^{-1}, and $J_2' = 8.6$ cm^{-1} (Scheme S1, ESI). The magnetically isolated Mn^{II} ion (Mn1B) was included in the Hamiltonian only as of the Zeeman component (Dz').

Isothermal magnetizations at 2 K (Figure S7, ESI) show that the saturation value (8.6 Nμ_B) for compound **2** is lower than that expected (10 Nμ_B). Strong antiferromagnetic coupling between the Mn^{II} and nitroxide ligand could be obtain from these results.

CONCLUSION

Co-crystal solids of types $[Mn(hfac)_2L^a_2\cdot Mn(hfac)_2L^a(H_2O)\cdot Mn(hfac)_2(H_2O)_2]$ (**1**) and $[Mn(hfac)_2L^b_2\cdot Mn(hfac)_2(H_2O)_2\cdot 0.5(C_6H_{14})]$ (**2**) were obtained that using NIT-Ph-(3-NIT) (L^a) and NIT-Ph-(3-NI) (L^b) as radical ligands to coordinate with $[Mn(hfac)_2](H_2O)_2$. The $[MnL_2]$ and [MnL] metal dications in each case coordinate the N−O$^\bullet$ group of one radical unit on a biradical, leaving the other uncoordinated radical unit. Crystallization water molecules play an essential role to assemble the overall solid-state structure in cocrystals **1** and **2**. Magnetically, relatively strong antiferromagnetic interactions between the cooperative radical teams and the manganese ion are dominant, with a lesser ferromagnetic exchange contribution from the radical−radical units within the biradical ligands. The exchange interactions from fragment A to B appear essentially small among the teams of radicals in compound **1**. Furthermore, the elaboration of similar structures is possible; this would provide extra prospects to take advantage of the different types of coordination sites, especially to form extended systems utilizing the relatively ferromagnetic exchange interaction provided by the *m*-phenylene biradical motif.

EXPERIMENTAL SECTION

Materials. All reagents were obtained from commercial sources and used as received.

Syntheses of Organic Biradicals. Biradicals were prepared using previously reported procedure with only minor modifications.[42,43]

Syntheses of Complexes $[Mn(hfac)_2L^a_2\cdot Mn(hfac)_2L^a(H_2O)\cdot Mn(hfac)_2(H_2O)_2]$ (1) and $[Mn(hfac)_2L^b_2\cdot Mn(hfac)_2(H_2O)_2\cdot 0.5(C_6H_{14})]$ (2). $Mn(hfac)_2\cdot 2H_2O$ (0.1 mmol) was dissolved in 15 mL of *n*-hexane and a few drops of ethanol. Then, 77.6 mg (0.2 mmol) of mixed biradicals dissolved in 2 mL of $CHCl_3$ was added with constant stirring. The solution was heated at 50−60 °C for 15 min, then stored in a dark room at room temperature. After 3 days, the reaction mixture was filtered, and a mixture of dark blue crystals (**1**) and orange crystals (**2**) was obtained. Analysis **1**: Found (%) C, 41.09; H, 3.55; N, 6.36. Calcd for $C_{90}H_{96}Mn_3F_{36}N_{12}O_{27}$ (%) C, 41.17; H, 3.54; N, 6.40. Analysis (**2**): Found (%) C, 42.72; H, 3.76; N, 6.36; C, 43.09; H, 3.55; N, 6.36. Calcd for $C_{63}H_{71}F_{24}Mn_2N_8O_{15}$ (%) C, 42.93; H, 3.97; N, 6.36. UV/vis spectrum of 0.1 mmol L^{-1} (**1** and **2**) in CH_2Cl_2.

Crystal Structure Determinations. Single crystals were selected to measure X-ray diffraction. The diffraction intensities of samples were collected using Bruker diffractometers, SMART-APEX II with a CCD and D8-QUEST with a CMOS area detector. Both kinds of crystals employed graphite-monochromated Mo Kα radiation ($\lambda = 0.71073$ Å) at 123 K. Data reductions were made using SAINT, and intensities were corrected for absorption by SADABS.[44,45] The direct methods with SHELXS-97 were used to solve the structures, and the structures were refined by full-matrix least-squares against F^2 using SHELXL.[46] Almost all hydrogen atoms were located from difference Fourier maps, and those not found were added at theoretical positions using the riding model. The selected crystal and refinement data are summarized in Table 1. More details can be obtained from the cif files, deposited at the Cambridge Crystallographic Data Centre and available free of charge on request via http://www.ccdc.cam.ac.uk/data_request/cif. The CCDC reference numbers are 2086025 and 2086026.

General Characterizations. Elemental analyses for C, H, and N were carried out using a PerkinElmer series II CHNS/O Analyzer 2400 at the Natural Science Center for Basic Research and Development (N-BARD), Hiroshima University. UV/vis spectra were recorded on a JASCO V-570 UV/vis/NIR spectrometer in the 200−800 nm range. The magnetization measurements were carried out on the single crystal with using Quantum Design MPMS-5S and MPMS-2 SQUID magnetometers. The magnetic field can be varied from −50 to 50 kOe,

https://doi.org/10.1021/acsomega.1c05285
ACS Omega 2022, 7, 10022−10028

and the temperature range is 2−300 K. The magnetic data were corrected for the sample diamagnetism according to Pascal's constants.[47]

■ ASSOCIATED CONTENT

Supporting Information

The Supporting Information is available free of charge at https://pubs.acs.org/doi/10.1021/acsomega.1c05285.

Magnetochemistry and detailed SC XRD experimental data (PDF)

Accession Codes

CCDC 2086025−2086026 contain the supplementary crystallographic data in the form of CIF files.

■ AUTHOR INFORMATION

Corresponding Authors

Yan-Li Gao − *School of Chemistry and Chemical Engineering, Yulin University, Yulin 719000, China;* orcid.org/0000-0001-7830-6016; Email: gaoyanli8503@126.com

Katsuya Inoue − *Department of Chemistry, Hiroshima University, Higashi-Hiroshima, Hiroshima 739-8526, Japan;* orcid.org/0000-0002-5542-3700; Email: kxi@hiroshima-u.ac.jp

Authors

Yufei Wang − *School of Chemistry and Chemical Engineering, Yulin University, Yulin 719000, China*

Liguo Gao − *School of Chemistry and Chemical Engineering, Yulin University, Yulin 719000, China*

Jian Li − *School of Chemistry and Chemical Engineering, Yulin University, Yulin 719000, China*

Yali Wang − *School of Chemistry and Chemical Engineering, Yulin University, Yulin 719000, China*

Complete contact information is available at: https://pubs.acs.org/10.1021/acsomega.1c05285

Notes

The authors declare no competing financial interest.

■ ACKNOWLEDGMENTS

This work was supported by a Grant-in-Aid for Scientific Research (S) (No. 25220803), Doctoral Scientific Research Foundation of Yulin University (No. 18GK24), Joint Fund of the Yulin University and the Dalian National Laboratory for Clean Energy (No. 2021007), Project of Shaanxi Provincial Department of Education (No. 20JC039), Social development projects of Shaanxi Science and Technology Department (No. 2020SF-408, 2021SF-449, and 2020QFY05-05), and Key R & D projects of Shaanxi Provincial Department of science and technology (No. 2021GY-165).

■ REFERENCES

(1) Gatteschi, D.; Coronado, E. Trends and challenges in molecule-based magnetic materials. *J. Mater. Chem.* **2006**, *16*, 2513−2515.

(2) Maspoch, D.; Domingo, N.; Ruiz-Molina, D.; Wurst, K.; Vaughan, G.; Tejada, T.; Rovira, C. J.; Veciana, J. A robust purely organic nanoporous magnet. *Angew. Chem., Int. Ed.* **2004**, *43*, 1828−1832.

(3) Allão, R. A.; Jordão, A. K.; Resende, J. A. L. C.; et al. Determination of the relevant magnetic interactions in low-dimensional molecular materials: the fundamental role of single crystal high frequency EPR. *Dalton Trans.* **2011**, *40*, 10843−10850.

(4) Luneau, D.; Rey, P. Magnetism of metal-nitroxide compounds involving bis-chelating imidazole and benzimidazole substituted nitronyl nitroxide free radicals. *Coord. Chem. Rev.* **2005**, *249*, 2591−2611.

(5) Baskett, M.; Paduan-Filho, A.; Oliveira, N. F.; Chandrasekaran, J. A.; Mague, J. T.; Lahti, P. M. Loops, Chains, Sheets, and Networks from variable coordination of $Cu(hfac)_2$ with a flexibly hinged aminoxyl radical ligand. *Inorg. Chem.* **2011**, *50*, 5060−5074.

(6) Inoue, K. *Struct. Bonding (Berlin)* **2001**, *100*, 61.

(7) Occharenko, V. *Stable Radicals*; John Wiely & Sons, 2010; p 461.

(8) Miller, J. S.; Drillon, M. *Magnetism: Molecules to Materials II: Molecule-Based Materials*; Wiely-VCH Verlag GmbH & Co, 2003; Chapter 1, p 1.

(9) Romanenko, G. V.; Maryunina, K. Yu.; Bogomyakov, A. S.; Sagdeev, R. Z.; Ovcharenko, V. I. Relationship between the thermally induced reorientations of aromatic solvate molecules in $Cu(hfac)_2$-nitroxide breathing crystals and the character of the magnetic anomaly. *Inorg. Chem.* **2011**, *50*, 6597−6609.

(10) Ratera, I.; Veciana, J. Playing with organic radicals as building blocks for functional molecular materials. *Chem. Soc. Rev.* **2012**, *41*, 303−349.

(11) Li, X.; Li, T.; Tian, L.; Liu, Z. Y.; Wang, X. G. A family of rare earth complexes with chelating furan biradicals: syntheses, structures and magnetic properties. *RSC Adv.* **2015**, *5*, 74864−74873.

(12) Lineberger, W. C.; Borden, W. T. The synergy between qualitative theory, quantitative calculations, and direct experiments in understanding, calculating, and measuring the energy differences between the lowest singlet and triplet states of organic diradicals. *Phys. Chem. Chem. Phys.* **2011**, *13*, 11792−11813.

(13) Train, C.; Norel, L.; Baumgarten, M. Organic radicals, a promising route towards original molecule-based magnetic materials. *Coord. Chem. Rev.* **2009**, *253*, 2342−2351.

(14) Ikoma, T.; Oshio, H.; Yamamoto, M.; Ohba, Y.; Nihei, M. Peculiarity in the electronic structure of Cu(II) complex ferromagnetically coupled with bisimino nitroxides. *J. Phys. Chem. A* **2008**, *112*, 8641−8648.

(15) Reis, S. G.; Briganti, M.; Martins, D. O. T. A.; Akpinar, H.; Calancea, S.; Guedes, G.; Soriano, S.; Andruh, M.; Cassaro, R. A. A.; Lahti, P. M.; Totti, F.; Vaz, M. G. F. First coordination compounds based on a bis(imino nitroxide) biradical and 4f metal ions: synthesis, crystal structures and magnetic properties. *Dalton. Trans.* **2016**, *45*, 2936−2944.

(16) Cerreia Vioglio, P.; Chierotti, M. R.; Gobetto, R. Pharmaceutical aspects of salt and cocrystal forms of APIs and characterization challenges. *Adv. Drug. Deliver. Rev.* **2017**, *117*, 86−110.

(17) Malamatari, M.; Ross, S. A.; Douroumis, D.; Velaga, S. P. Experimental cocrystal screening and solution based scale-up cocrystallization methods. *Adv. Drug. Deliver. Rev.* **2017**, *117*, 162−177.

(18) Douroumis, D.; Ross, S. A.; Nokhodchi, A. Advanced methodologies for cocrystal synthesis. *Adv. Drug. Deliver. Rev.* **2017**, *117*, 178−195.

(19) Vaz, M. G. F.; Akpinar, H.; Guedes, G. P.; Santos, S.; Novak, M. A.; Lahti, P. M. Two co-crystalline $M(hfac)_2(IPhIN)_2$ $M(hfac)_2$ (M = Mn, Co) compounds with a bis(iminoylnitroxide) biradical: structure and magnetism. *New. J. Chem.* **2013**, *37*, 1927−1932.

(20) Gao, Y. L.; Maryunina, K. Y.; Hatano, S.; Nishihara, S.; Inoue, K.; Kurmoo, M. Co-crystallization of achiral components into chiral network by supramolecular interactions: coordination complexes-organic radical. *Cryst. Growth. Des.* **2017**, *17*, 4893−4899.

(21) Caneschi, A.; Chiesi, P.; David, L.; Ferraro, F.; Gatteschi, D.; Sessoli, R. Crystal structure and magnetic properties of two nitronyl nitroxide biradicals and of their copper(II) complexes. *Inorg. Chem.* **1993**, *32*, 1445−1453.

(22) Shiomi, D.; Tamura, M.; Katori, H. A.; Goto, T.; Hayashi, A.; Ueda, Y.; Sawa, H.; Kato, R.; Kinoshita, M. Magnetic structure of the 4,4,4′,4′,5,5,5′,5′-octamethyl-2,2′-m-phenylenebis(4,5-dihydroimida-

zol-1-oxyl 3- oxide) biradical: quantum spin effect of S = 1 species associated with structural change. *J. Mater. Chem.* **1994**, *4*, 915−920.
(23) Catala, L.; Le Moigne, J.; Kyritsakas, N.; Rey, P.; Novoa, J. J.; Turek, P. Towards a better understanding of the magnetic interactions within *m*-Phenylene α-Nitronyl Imino nitroxide based biradicals. *Chem.—Eur. J.* **2001**, *7*, 2466−2480.
(24) Titi, H. M.; Kelley, S. P.; Easton, M. E.; Emerson, S. D.; Rogers, R. D. Formation of ionic co-crystals of amphoteric azoles directed by the ionic liquid co-former 1-ethyl-3-methylimidazolium acetate. *Chem. Commun.* **2017**, *53*, 8569−8572.
(25) Duggirala, N. K.; Perry, M. L.; Almarsson, Ö.; Zaworotko, M. J. Pharmaceutical cocrystals: along the path to improved medicines. *Chem, Comm.* **2016**, *52*, 640−655.
(26) Wang, X. P.; Chen, W. M.; Qi, H.; et al. Solvent-controlled phase transition of a Co^{II}-organic framework: from achiral to chiral and two to three dimensions. *Chem.—Eur. J.* **2017**, *23*, 7990−7996.
(27) Tanaka, A.; Inoue, K.; Hisaki, I.; Tohnai, N. A.; et al. Supramolecular chirality in layered crystals of achiral ammonium salts and fatty acids: a hierarchical interpretation. *Angew. Chem., Int. Ed.* **2006**, *45*, 4142−4145.
(28) Shan, N.; Zaworotko, M. J. The role of cocrystals in pharmaceutical science. *Drug. Discovery. Today.* **2008**, *13*, 440−446.
(29) Rodríguez-Hornedo, N.; Nehm, S. J.; Jayasankar, A. Cocrystals: design, properties and formation mechanisms, In *Encyclopedia of Pharmaceutical Technology*, 3rd ed.; Taylor & Francis: London, 2007; p 615.
(30) Bolton, O.; Matzger, A. J. Improved stability and smart-material functionality realized in an energetic cocrystal. *Angew. Chem. Int. Ed* **2011**, *50*, 8960−8963.
(31) Caneschi, A.; Gatteschi, D.; Le Lirzin, A. Crystal structure and magnetic properties of a new ferrimagnetic chain containing manganese(II) and a nitronyl-nitroxide radical. Magnetic ordering in $Mn(hfac)_2NITR$ compounds. *J. Mater. Chem.* **1994**, *4*, 319−326.
(32) Liu, Z. L.; Zhao, Q. H.; Li, S. O.; Liao, D. Z.; Jiang, Z. H.; Yan, S. P. Structure and magnetic properties of ferrimagnetic chain formed by manganese(II) and nitronyl nitroxides. *Inorg. Chem. Commun.* **2001**, *4*, 322−325.
(33) Vaz, M. G. F.; Allão, R. A.; Akpinar, H.; Schlueter, J. A.; Santos, S., Jr; Lahti, P. M.; Novak, M. A. Magnetic Mn and Co complexes with a large polycyclic aromatic substituted nitronyl nitroxide. *Inorg. Chem.* **2012**, *51*, 3138−3145.
(34) Osiecki, J. H.; Ullman, E. F. Studies of free radicals. I..alpha.-Nitronyl nitroxides, a new class of stable radicals. *J. Am. Chem. Soc.* **1968**, *90*, 1078−1079.
(35) Azuah, R. T.; Kneller, L. R.; Qiu, Y.; Tregenna-Piggott, P. L. W.; Brown, C. M.; Copley, J. R. D.; Dimeo, R. M. DAVE: A Comprehensive Software Suite for the Reduction, Visualization, and Analysis of Low Energy Neutron Spectroscopic Data. *J. Res. Natl. Inst. Stand. Technol.* **2009**, *114*, 341−358.
(36) Li, H. D.; Sun, J.; Yang, M.; Sun, Z.; Tang, J. K.; Ma, Y.; Li, L. C. Functionalized Nitronyl Nitroxide Biradicals for the Construction of 3d-4f Heterometallic Compounds. *Inorg. Chem.* **2018**, *57*, 9757−9765.
(37) Catala, L.; Le Moigne, J.; Kyritsakas, N.; Rey, P.; Novoa, J. J.; Turek, P. Towards a Better Understanding of the Magnetic Interactions within m-Phenylene α-Nitronyl Imino Nitroxide Based Biradicals. *Chem. - Eur. J.* **2001**, *7*, 2466−2480.
(38) Dickman, M. H.; Porter, L. C.; Doedens, R. J. Bis(nitroxyl) adducts of bis(hexafluoroacetylacetonato)manganese(II). Preparation, structures, and magnetic properties. *Inorg. Chem.* **1986**, *25*, 2595−2599.
(39) Kahn, O. *Molecular Magnetism*; Wiley-VCH: Weinheim, Germany, 1993.
(40) Biswas, A.; Drew, M. G. B.; Gómez-Garcia, C. J.; Ghosh, A. Use of a reduced schiff-Base ligand to prepare novel chloro-bridged chains of rare Cu(II) trinuclear complexes with mixed azido/oxo and chloro/oxo bridges. *Inorg. Chem.* **2010**, *49*, 8155−8163.
(41) Ma, Y.; Wen, Y. Q.; Zhang, J. Y.; Gao, E. Q.; Liu, C. M. Structures and magnetism of azide- and carboxylate-bridged metal(II) systems derived from 1,2-bis(*N*-carboxymethyl-4-pyridinio)ethane. *Dalton. Trans.* **2010**, *39*, 1846−1854.
(42) Hirel, C.; Vostrikova, K. E.; Pecaut, J.; Ovcharenko, V. I.; Rey, P. Nitronyl and imino nitroxides: improvement of ullman's procedure and report on a new efficient synthetic soute. *Chem. Eur. J.* **2001**, *7*, 2007−2014.
(43) Ullman, F. E.; Osiecki, J. H.; Boocock, D. G. B.; Darcy, R. Stable free radicals. X. Nitronyl nitroxide monoradicals and biradicals as possible small molecule spin labels. *J. Am. Chem. Soc.* **1972**, *94*, 7049−7059.
(44) *SAINT-Plus*, version 6.02, Bruker Analytical X-ray System, Madison, WI, 1999.
(45) Sheldrick, G. M. *SADABS - An empirical absorption correction program*; Bruker Analytical X-ray Systems, Madison, WI, 1999.
(46) Sheldrick, G. M. Crystal structure refinement with SHELXL. *Acta Crystallogr. Sect. C: Struct. Chem.* **2015**, *71*, 3−8.
(47) Boudreaux, E. A.; Mulay, L. N. *Theory and application of molecular paramagnetism*; John Wiley & Sons, New York, 1976; p 491.

https://doi.org/10.1021/acsomega.1c05285
ACS Omega 2022, 7, 10022−10028